analytical chemistry

Article

pubs.acs.org/ac

Second Harmonic Generation Guided Raman Spectroscopy for Sensitive Detection of Polymorph Transitions

Azhad U. Chowdhury,[†] Dong Hye Ye,[‡] Zhengtian Song,[†] Shijie Zhang,[†] Hartmut G. Hedderich,[†] Babita Mallick,[§] Satyanarayana Thirunahari,[§] Srividya Ramakrishnan,[§] Atanu Sengupta,[§] Ellen J. Gualtieri,[∥] Charles A. Bouman,[‡] and Garth J. Simpson*[,†]

[†]Department of Chemistry, Purdue University, 560 Oval Drive, West Lafayette, Indiana 47907, United States

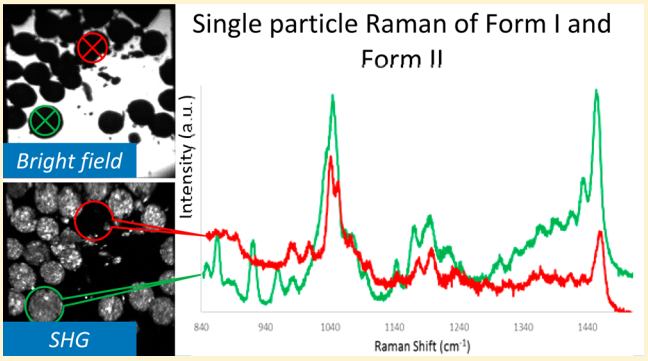
[‡]Department of Electrical and Computer Engineering, Purdue University, 465 Northwestern Avenue, West Lafayette, Indiana 47907, United States

[§]Dr. Reddy's Laboratories, IPDO, Bachupally Campus, Hyderabad, Telengana 500090, India

[∥]Formulatrix, Inc. 10 DeAngelo Drive, Bedford Massachusetts 01730, United States

Supporting Information

ABSTRACT: Second harmonic generation (SHG) was integrated with Raman spectroscopy for the analysis of pharmaceutical materials. Particulate formulations of clopidogrel bisulfate were prepared in two crystal forms (Form I and Form II). Image analysis approaches enable automated identification of particles by bright field imaging, followed by classification by SHG. Quantitative SHG microscopy enabled discrimination of crystal form on a per particle basis with 99.95% confidence in a total measurement time of ∼10 ms per particle. Complementary measurements by Raman and synchrotron XRD are in excellent agreement with the classifications made by SHG, with measurement times of ∼1 min and several seconds per particle, respectively. Coupling these capabilities with at-line monitoring may enable real-time feedback for reaction monitoring during pharmaceutical production to favor the more bioavailable but metastable Form I with limits of detection in the ppm regime.



Crystal form and polymorph transitioning can profoundly affect the stability and bioavailability of active pharmaceutical ingredients (APIs). Polymorphism refers to the existence of multiple crystalline solid forms of identical composition, with this multiplicity arising from the packing and/or the relative orientation of molecules in the crystal lattice. These differences in crystal lattice of an API generally exhibit different bioavailability by differing their physicochemical properties such as dissolution kinetics, thermodynamic stability, etc.[1−4] A classic example is the case of ritonavir, in which the marketed final dosage form spontaneously converted to a more stable and previously unknown crystal form, which exhibited substantially slower dissolution kinetics and correspondingly lower bioavailability.[5] A recent study estimates that more than 80% of APIs have multiple known polymorphic forms.[6]

Clopidogrel bisulfate is a particularly interesting example, in which seven different polymorphic form have been identified; among them only Form I and Form II are used for the drug formulation.[7−9] Clopidogrel bisulfate is a drug that falls into thienopyridine class. It inhibits platelet aggregation and is used to treat patients with acute coronary syndrome. Only the dextrorotatory enantiomer exhibits antiplatelet aggregation where the levorotatory enantiomer remains inactive,[10] and therefore the final dosage form is typically a pure enantiomeric form preparation. The Form I polymorph is metastable, but exhibits significantly higher bioavailability than the more thermodynamically stable Form II.[8] Solvent mediated crystallization is the most common method for the production of clopidogrel bisulfate for pharmaceutical materials, in which the desired Form I is kinetically the first to be produced, followed by spontaneous transformation to Form II if the reaction is allowed to progress. Both polymorphic forms of clopidogrel bisulfate possess an enantiotropic system where two different polymorphs are stable at different temperatures; thus Form I has the potential to spontaneously transition to the more stable Form II during manufacture and storage.[9,11] Therefore, methods capable of sensitively identifying the early onset of the Form I to Form II transition could be used for active control to ensure Form I production during synthesis and storage. Even a small mass fraction of the more stable polymorph may negatively impact the dissolution kinetics by

Received: February 3, 2017
Accepted: May 8, 2017
Published: May 8, 2017

© 2017 American Chemical Society

DOI: 10.1021/acs.analchem.7b00431
Anal. Chem. 2017, 89, 5958−5965

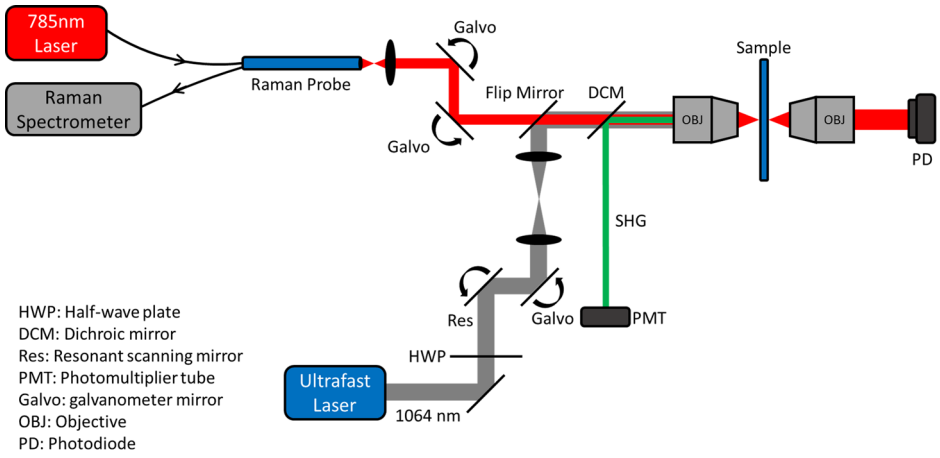


Figure 1. Schematic diagram of Raman spectroscopy integrated SHG microscope.

serving to nucleate precipitation of the API upon introduction to the gut.[12]

The Food and Drug Administration (FDA) and other government agencies require thorough characterization of APIs during filing for a new drug applications (NDAs) and abbreviated new drug applications (ANDAs).[2,13,14] High-throughput (HT) analytical methods for APIs screening are advantageous, spanning the early stages of drug development through to assessment of the shelf life of final dosages. Assessments of composition are typically performed by batch sampling, in which analysis of representative aliquots is used to assess composition during reaction. Several analytical methods have been explored for clopidogrel polymorphic form characterization and quantification including powder X-ray diffraction (PXRD) analysis,[15] vibrational spectroscopic technique combined with chemometrics,[9] solid state stress degradation studies,[16] and X-ray microtomography.[17] In PXRDs, Uvarov and Popov have quantified the clopidogrel phase content in the mixture of Form I and Form II using X-ray powder pattern decomposition and classical direct methods. The limit of detection was found to be 1.0−1.5 wt % in both methods.[15] In another quantitative analysis of clopidogrel bisulfate Form II in Form I, Nemet and co-workers combined IR and Raman spectroscopy with chemometrics and quantified 2% and 3% of Form II in Form I, respectively, with less than 1% limit of detection.[9] Recently, a microscopy based approach combined with image-analysis was developed to extract morphological details for quantification of trace amount of polymorphic phases. In this study, a synchrotron radiation X-ray computed microtomography (SR-μCT) was used for selective and sensitive detection of clopidogrel bisulfate polymorphs. The limit of detection (LOD) was also found to be 1%.[17] Although, this microscopy based approach shows good promise in polymorphic phase determination in terms of required time to the sample a large area (2048 × 2048 pixels in 2 s, pixel size = 3.7 μm), it is not suitable for online phase monitoring due to the requirement of a synchrotron radiation source. Although, these reported techniques are capable of detecting polymorphic phases down to ∼1% LOD, none of these techniques possesses enough sensitivity to reach LOD into the parts per million (ppm) regime relevant to kinetic modeling of stability and dissolution kinetics.

Recent studies have suggested the use of nonlinear optical imaging for quantifying both overall crystalline content and crystal polymorphism in pharmaceutical formulations. The results of these studies have shown the capabilities of nonlinear optical imaging to detect organic nanocrystal,[18] quantify second order nonlinear optical signal from various active pharmaceutical ingredients,[19,20] detect and characterize metastable polymorphs,[21,22] discriminate polymorphs rapidly,[23] detect crystallinity in ppm regime,[24] and quantify second order nonlinear optical signal per particle basis in powder matrix.[25] Previous studies suggested nonlinear optical methods can be used for discrimination of crystal forms in model systems with well-defined polymorphs, and definitive confirmation has not yet been demonstrated through independent analyses on pharmaceutically relevant materials.

The general applicability of SHG for pharmaceutical materials analysis has been bolstered by the increasing use of homochiral small molecules in formulations. The large majority of new small molecule active pharmaceutical ingredients are homochiral, with one or more chiral center.[26] With the exception of a few relatively rare high-symmetry systems, the remaining common space groups into which a small chiral molecule can crystallize are symmetry-allowed for SHG-activity.[27] The relaxation of phase-matching requirements in SHG microscopy allows for reasonably reliable *ab initio* prediction of the SHG activities of both small molecule and large molecule crystals from the known packing arrangements.[20,28] Such calculations can help inform the potential appropriateness of SHG-guided analysis prior to experimental studies and to obtain an initial estimate of the anticipated difference in SHG activity for different polymorphic forms.

In this work, we propose the use of Raman and synchrotron PXRD guided by SHG microscopy for crystal form characterization of individual ∼100 ng particles of clopidogrel bisulfate. Specifically, the combination of bright field imaging and SHG microscopy was used to identify candidate particles for subsequent Raman and PXRD analysis of crystal form. Measurements are presented for physical mixtures of Form I and Form II particles, prepared similarly with the exception of the reaction time; the reaction time was extended for the Form II production to allow complete transitioning.

EXPERIMENTAL SECTION

Materials and Sample Preparation. Pure clopidogrel bisulfate Form I and Form II were produced in-house at Dr. Reddy's Lab. As produced, both polymorphic forms were

DOI: 10.1021/acs.analchem.7b00431
Anal. Chem. 2017, 89, 5958−5965

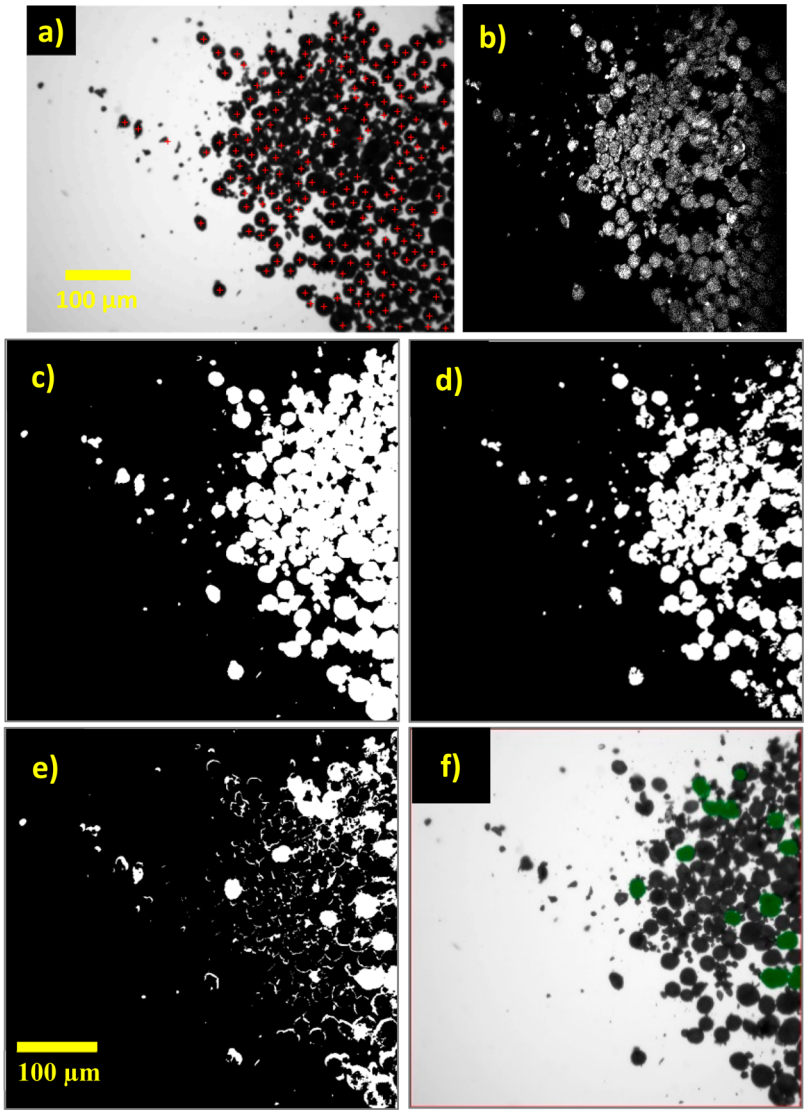


Figure 2. Representation of the segmentation algorithm to perform classification of individual particles. Brightfield (3a) and SHG (3b) images are shown for a mixture of clopidogrel bisulfate (10% Form II/90% Form I). Red cross-hairs in the image indicate the representative candidates for the polymorphic form classification. The images in parts a and b were brought into the registry and converted to binary images in parts c and d, respectively, to identify (i) the locations of all the particles and (ii) the locations of the SHG-dim fraction. The difference map shown in part e allows classification of the Form II particles, indicated by the green circles in part f.

generated as white spherical particles, exhibiting a similar size distribution with a diameter of ∼25 μm as determined by calibrated bright field image analysis. Samples was prepared as powdered blends consisting of 10% clopidogrel bisulfate Form II in Form I by mass. Images were taken for powders compacted between two glass microscope slides from at least three arbitrarily chosen locations of each sample to provide representative sampling.

SHG Imaging. SHG micrographs were obtained using a commercial Formulatrix SONICC system, modified in-house for compatibility with powder analysis. In brief, a Fianium femtosecond laser was used as the incident source (170 fs, 1.3 W, 1060 nm, 51 MHz repetition rate). SHG images were produced by beam-scanning through a 10× objective with a ∼2 mm × 2 mm field of view with the SHG measured in transmission. Unless otherwise indicated, 150 mW laser power measured at the sample and 1 s image acquisition time was used for SHG imaging. Bright field images acquired with a white-light source and a camera in the same instrument were used to identify particle locations by segmentation algorithms described in detail in a subsequent section.

SHG Guided Raman Measurement. A prototype built-in-house microscope was used to acquire Raman spectra from SHG active and inactive particles in each field of view. In this prototype instrument, output of a Toptica continuous wave (CW) laser (785 nm wavelength) was collected by an optical fiber of a custom-made Raman probe (InPhotonics, RPS785/24), shown in Figure 1, and recollimated by a 1/2 in. fused silica lens. Collimated light then taken through a scan head followed by two other fused silica 1 in. lenses in a 4f configuration to focus on the sample using a 10× objective. A galvanometer mirror pair was used in the scan head and precise voltage controlling on two galvanometer mirrors rapidly drives the Raman beam to a location of choice in each field of view. Using of two galvanometer mirrors was advantageous in a way that it also could be used to scan the sample for spectral imaging. Raman signal from the sample was collected in epi, following the same beam path back through the same Raman

DOI: 10.1021/acs.analchem.7b00431
Anal. Chem. 2017, 89, 5958−5965

probe and directed into a Raman spectrometer (SpectraPro 300i, Acton Research) to generate the spectrum. There was a built-in notch filter in the probe to reject the laser line. A 100 × 1340 CCD array was used for spectral detection employing vendor software (Winspec32). Two different computers were used in this prototype instrument, one to drive the beam and the other to collect the spectrum.

X-ray Diffraction Measurement. X-ray diffraction (XRD) measurements were carried out using a SHG integrated XRD multimodal microscope in Argonne National Laboratory. Instrument details are described elsewhere.[29,30] In short, a Fianium FemtoPower ~1060 nm ultrafast fiber laser that generated ~160 fs pulses centered at 1064 nm, with a 50 MHz repetition rate was integrated into the GM/CA@ APS beamline 23-ID-B at the Advanced Photon Source. The infrared beam was scanned across the sample through a 10× objective with a numerical aperture (NA) of 0.3 using a resonant scanner and a galvanometer mirror. SHG and bright field images of the transmitted infrared beam were collected in transmission. An unattenuated photon flux with a photon energy of 12 keV, 5 μm diameter beam was used to generate X-ray scattering patterns from highly confined locations. XRD patterns were acquired with 2 s exposure time per location with another 2 s for dead time between next exposure in a 4 × 4 grid.

Image Segmentation and Registration. An image segmentation algorithm was developed and written in Matlab, in which a normalized cross correlation (NCC) based template matching algorithm was trained by images of a 1951 USAF resolution test chart taken by two different modalities: bright field and SHG. In the following step, Otsu's adaptive thresholding was applied to SHG images to create binary masks (Figure 2d). Assuming two polymorphs are present, a bimodal intensity distribution in intensity is expected. Otsu's method separates image into two classes, i.e., background and foreground; the algorithm starts with an arbitrary threshold then searches for an optimal threshold that maximizes the interclass variance.[31] A binary image was also created (Figure 2c) using the bright field image followed by removal of residual pixels to match the SHG image dimensions. Subtraction followed by pruning the residual mask recovered the particles that produced low SHG signals (Figure 2f), identified as the Form II polymorph.

RESULTS AND DISCUSSION

Pure Sample Measurement. SHG images were obtained from the pure Form I and Form II powders, the results are presented in Figure 2. Form I exhibit ~250 times higher SHG activity per unit volume than Form II. The integrated intensity over multiple z-planes (Figure 3) totaling a depth of field ~120 μm was divided by the estimated volume of an individual particle multiplied with the total number of the particles in the field of view to determine the SHG activity per unit volume, normalized to a reference material of point-source $BaTiO_3$ nanoparticles (500 nm). The diameters of particles were calculated from the bright field measurements and the SHG activities per particle were recovered using the segmentation algorithm. The combined mean and standard deviation in the SHG activities on per particle basis were 35 ± 9 counts/μm^2 for Form I and 0.095 ± 0.003 counts/μm^2 for Form II. In general, higher symmetry crystals tend to produce weaker SHG activity,[28] consistent with the observed trends for clopidogrel bisulfate. Clopidogrel bisulfate Form I is known to adopt a monoclinic unit cell and belongs to the $P2_1$ space group, and

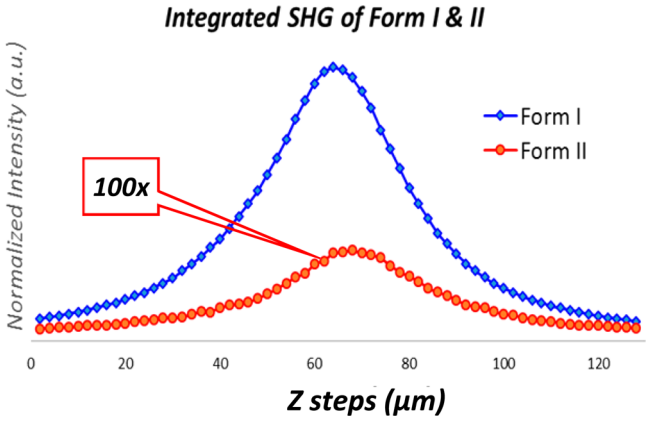


Figure 3. Integrated SHG intensity measured as the focal plane was translated through powders of Form I and Form II CB. The integrated SHG intensity from Form II was rescaled by 100-fold to aid in visualization. Outliers (bright SHG puncta in Form II) were excluded in this calculation.

Form II has an orthorhombic unit cell and belongs to the $P2_12_12_1$ space group.[15] Assuming a normal distribution of uncertainty, individual particles can be assigned to either Form I or Form II with a statistical confidence of 99.995% based solely on their differences in SHG activity.

Form I and Form II Mixtures. In order to quantify polymorphic phase content in a mixture, bright field and SHG images were taken for a 10% mixture of Form II in Form I. The combination of bright-field and SHG micrographs provided a means to make initial classifications of individual particles as either Form I or Form II, the process of which is illustrated in Figure 2. Bright field images enabled identification of particle locations with a high signal-to-noise ratio (SNR), while the difference in SHG per unit volume (SHG/V) for Forms I and II was used for initial classification of the crystal form. Since the bright field and SHG images were acquired using independent beam paths, image registration algorithms were developed and employed to correct for the disparities in the number of pixels and in the fields of view for the two imaging modalities as described in the Experimental Section. The assumption of spheroidal particle morphologies (~25 μm in diameter) reduced complications from particle−particle overlap in the segmentation algorithm.

Raman Spectroscopy for Crystal Form Discrimination. Following the initial classification by SHG, independent assessment of the crystal form was performed by Raman spectroscopy using the SHG/V analysis to guide selection of relevant particles of interest, the results of which are presented in Figure 4. Figure 4a and 4b correspond to the postprocessed bright field image and SHG image, respectively. Representative Form II candidates are indicated by the red (SHG activity, low) and Form I candidates by blue (SHG activity, high) circles in both images. In order to acquire a Raman spectrum from each particle, the appropriate position of the Raman acquisition was selected by a galvanometer mirror pair and Raman scattering from the targeted particles was integrated for ~1 min (2 s per frame for 30 frames) to generate high SNR spectra. Excellent agreement was observed between the Form II reference spectrum and the Raman spectrum of individual ~100 ng particles classified as Form II based on the combined bright-field and SHG/V assessments. Similarly, definitive agreement was also observed for the Form I reference spectra with those

DOI: 10.1021/acs.analchem.7b00431
Anal. Chem. 2017, 89, 5958−5965

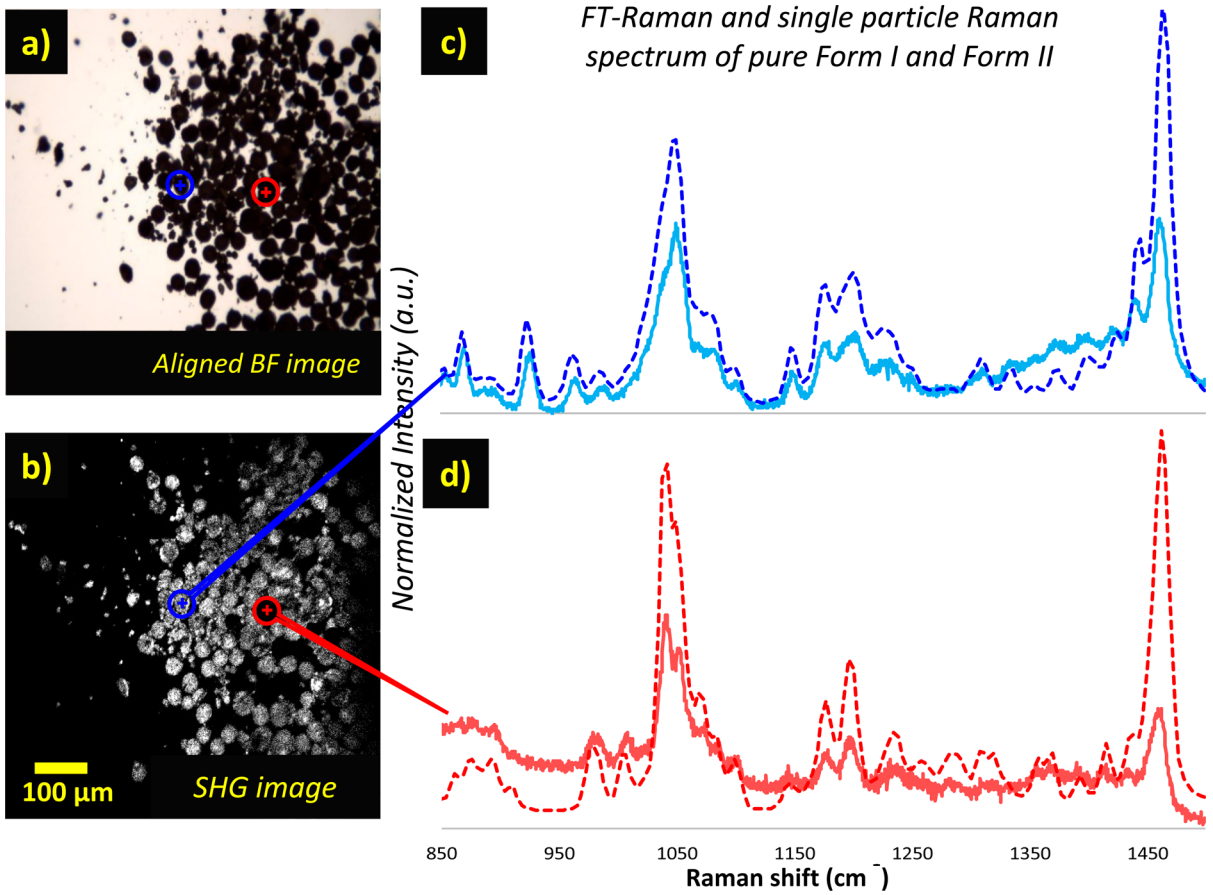


Figure 4. Crystal form classification by independent SHG-guided Raman analysis on a per-particle basis. Parts a and b correspond to bright field and SHG images of a 10% mixture of Form II in Form I, respectively. Parts c and d correspond to single particle Raman spectrum and FT-Raman spectrum, respectively, of Form I and Form II. FT-Raman spectra of both Forms are shifted a few wavenumbers to the right to match the spectra feature collected from single particle measurements. In both cases, Raman spectra support the preliminary classifications made by SHG microscopy.

obtained from particles classified as Form I in 10% mixture sample.

X-ray Diffraction for Further Validation. In addition to the Raman measurements, SHG guided synchrotron XRD measurements were also performed (Figure 5) for the 10% mixture to assess the capabilities of single-particle assessments of crystal form by SHG. Figure 5a is the laser transmittance image of the 10% mixture, yellow circles in this image indicate the Form I and Form II identified by the SHG/V measurement. A collimated X-ray beam, 5 μm in diameter, was used to raster the particle (shown in the inset of Figure 5b,d). The use of a narrow 5 μm X-ray "mini-beam" enhanced the sensitivity of the measurement from localized sampling and corresponding background reduction. Diffraction images from each raster scan were integrated to make a single diffraction image. Combinations of diffraction images interrogate a broader window of particle's crystallographic orientation distribution thus suitable for statistical average, assuming the particles orientation were uniformly distributed. An integration of intensities along the azimuthal angle of a diffraction image recovers the anticipated powder X-ray diffraction (PXRD) pattern. Experimental diffraction patterns were also compared to the theoretical predictions of the monoclinic and orthorhombic unit cell, obtained from Cambridge Structural Database (CSD) for Form I and Form II, respectively, shown in Figure 5.

Combining the segmentation with SHG measurements allows identification of particles of interest based on the differences in the SHG/V. From the results in Figure 3, significant differences are expected for the Form I and Form II polymorphs. Statistical analysis of the integrated SHG activity per particle basis of both forms suggests a discriminatory confidence of 99.995% based on SHG alone. However, these results are only valid if the dominant differences are definitively connected directly to polymorphism, rather than other physical differences within the particles (e.g., crystal size distribution, orientation, degree of crystalline order, etc.). Roughly comparable confidence arises in both the Raman and PXRD analyses. Because the other spectroscopic methods are based on unique physical properties, the overall rate of misclassification is given by the product of the independent rates (for example, a misclassification probability of 0.005% by SHG and 0.1% by Raman would result in a combined misclassification probability of one part in 2×10^7).

All three approaches (SHG, Raman, PXRD) provided excellent discriminatory capabilities for crystal form characterization. In the case of SHG, >99.99% confidence was achieved on a per-particle basis through the combination bright field for particle localization and average SHG for crystal form determination. Qualitatively similar trends were clearly observed by both Raman and XRD. While SHG enables this discrimination from a single scalar input (SHG/V), both the Raman and XRD carry additional structural information

DOI: 10.1021/acs.analchem.7b00431
Anal. Chem. 2017, 89, 5958−5965

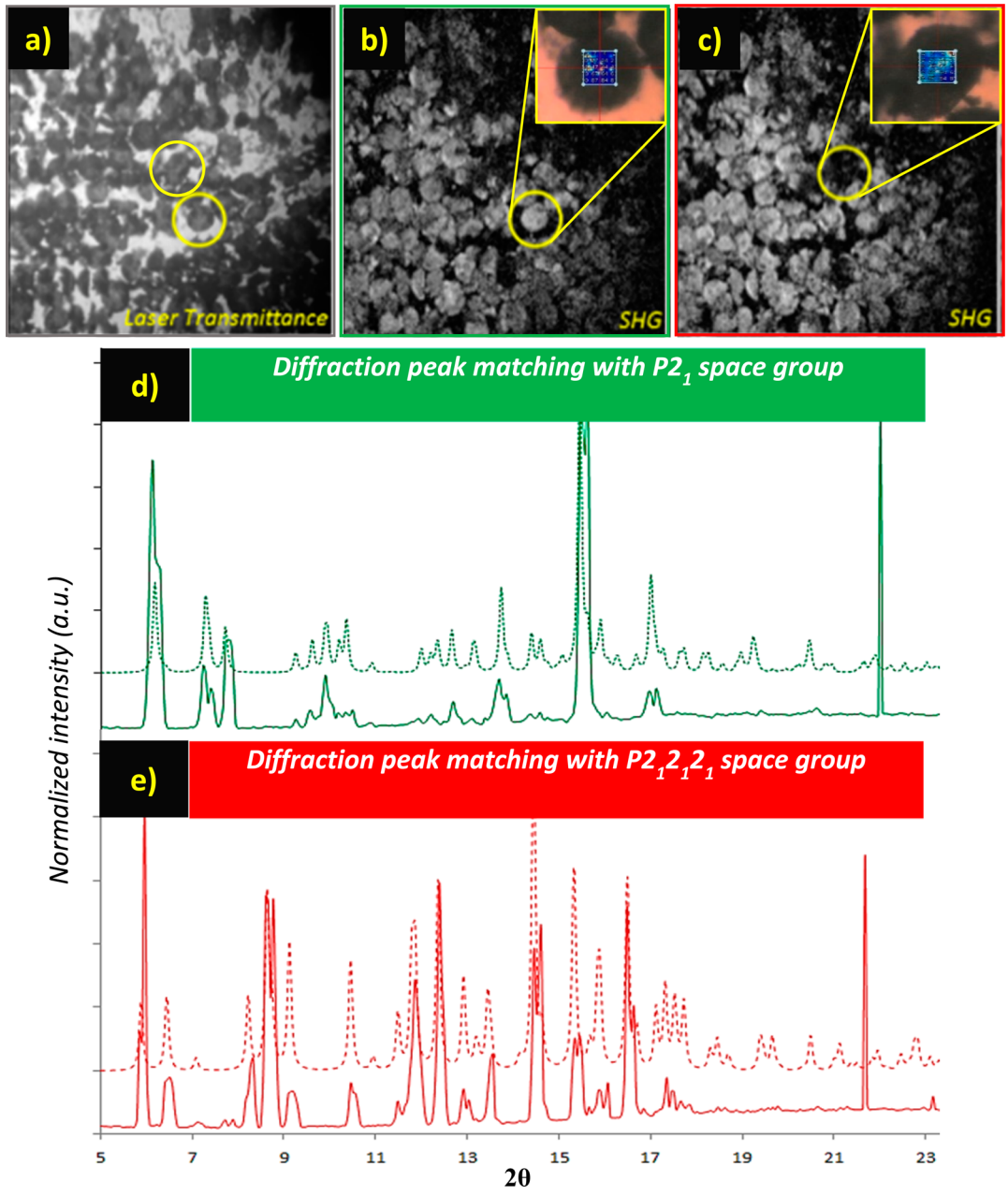


Figure 5. Initial classification by SHG/V measurement of 10% physical mixture of Form II in Form I and independent evaluation by PXRD measurement. Image a corresponds to the bright field image of 1% mixture, and images b and c correspond to the SHG image of the same field of view. The yellow circles indicate SHG-bright and SHG-dim particles selected as candidates for the diffraction measurements. Experimental powder diffraction patterns from those particles are compared to the theoretical prediction for Form I and Form II in parts d and e, respectively.

through the recovered spectra (1D) and scattering patterns (2D). However, the greatest discrimination capabilities result from dimension reduction to a single scalar value to optimally inform crystal form, such that the measurement objectives are ultimately based on qualitatively similar inputs.

While all three methods allowed high degrees of crystal form discrimination, SHG microscopy has clear benefits in terms of simplicity and measurement time. In practice, conventional Raman required >several seconds of signal acquisition per particle to obtain spectra with sufficient SNR for highly confident crystal form discrimination, since the spontaneous Raman event is relatively inefficient (1 in 10^7 Raman scattering events relative to Rayleigh scattering).[32] For a spectral acquisition time of 60 s, a mixture of 1% Form II would take ~15 h of continuous signal acquisition from 900 individual particles followed by post processing of these spectra to quantify polymorphic phase content (assuming no dead time and detection of 9 Form II particles for an SNR = 3 from Poisson statistics). The time frame for synchrotron analysis is considerably reduced, with as little as 1 s integration time per particle, corresponding to ~30 min of acquisition (assuming 1 s dead time for data transfer and sample repositioning). However, synchrotron time is also considerably more difficult to routinely access, given the high demands on beam-time and limited number of synchrotron facilities. In contrast, SHG imaging allowed characterization of all particles within a 1 × 1 mm^2 area with 1 s of data acquisition. For an average of ~200 particles in a given field of view, the time frame required to

DOI: 10.1021/acs.analchem.7b00431
Anal. Chem. 2017, 89, 5958−5965

probe 900 particles is still only a few seconds. To achieve LOD of 0.1% would require ~1 min (40 frames with ~0.5 s dead time for sample repositioning between frames), and 100 ppm would still only require ~10 min.

The relatively low variance in the SHG intensity per particle is consistent with the presence of numerous small crystallites within each spheroidal particle. The relative standard deviation (RSD) in the SHG/V determination for both Forms I and II was ~15% (calculated from more than 100 particles taken from different fields of view, yielding 35 ± 9 counts/μm^2 for Form I and 0.095 ± 0.003 counts/μm^2 for Form II). The low relative RSD observed in this study contrasts significantly from SHG microscopy measurements in powders, in which the RSD approached unity for a uniformly distributed population of $BaTiO_3$ nanoparticles.[25] The low per particle RSD is consistent with individual particles comprised of polycrystalline conglomerate, rather than single crystals. For a polycrystalline conglomerate, a representative population of numerous small crystallites contributes to the overall SHG intensity observed, rather than a few relatively large sources. In the limit of the average crystal size being much less than the focal volume, a statistical population of all sizes and orientations is sampled within each individual particle, reducing the particle-to-particle variance in SHG intensity.

It is important to note that the classification of crystal form on a per-particle basis implicitly assumes that individual particles will be present as either Form I or Form II, rather than a mixture containing both forms in each particle. In practice, it is well established that the kinetics of phase transformation are significantly faster for intraparticle interactions,[33,34] in which adjacent crystalline domains are in intimate contact within the particle and can serve to nucleate Form II conversion, relative to interparticle interactions involving minimal and transient crystal contact. As such, kinetically it is reasonable to assume that any initial nucleation event in a given particle results in rapid transition throughout the extent of the particle but slow (if any) propagation to adjacent particles, consistent with the expectations of the analysis.

It is also worth considering the ability of SHG alone to discriminate between the relatively weak Form II and the SHG-inactive amorphous form of clopidogrel bisulfate. While Form II particles do produce SHG significantly greater than amorphous materials, the signals are sufficiently weak that discrimination between amorphous versus Form II particles may be challenging. Fortunately, two strategies can help inform such decisions. First, reaction monitoring is typically performed throughout the entire time-course of the reaction, such that the kinetics associated with crystal formation and transitioning could provide additional insights into the most likely composition of a particle exhibiting weak SHG activity. However, more reliable assignments could be made by integration of Raman spectroscopy with SHG to guide the analysis to the particles of greatest interest.

In light of these collective metrics, SHG-guided Raman can potentially combine the advantages of both high speed and chemical specificity. In cases in which the composition is clear-cut from SHG alone, confident assessments of crystal form can be made rapidly on a per-particle basis. In ambiguous cases where classification by SHG alone lacks high statistical confidence, those particular particles can be flagged for subsequent analysis by Raman spectroscopy, maximizing the utilization of the information-rich but time-consuming spectroscopic analysis.

CONCLUSIONS

In this study, a prototype instrument (SHG microscopy guided Raman spectroscopy and powder X-ray diffraction) was used to confirm the rapidly identified trace polymorphic form of clopidogrel bisulfate Form II in Form I by SHG measurement. Measurement validations are presented for physical mixtures of Form I and Form II particles. The combination of bright field imaging and SHG microscopy was used to identify candidate particles for subsequent Raman and PXRD analysis of crystal form. Both the SHG guided Raman and synchrotron PXRD results support the initial tentative assignments of the crystal form by SHG. Nevertheless, additional benefits of combining methods for orthogonal determination, SHG guiding provides a huge time-saving and enhanced sensitivity by excluding particles that are unlikely to be Form II based on the presence of bright SHG. At the same time, quantification of polymorphic phase content becomes very straightforward by rejecting the requirement of a calibration plot that is required for any other quantitative analytical method. This study potentially can improve overall yield and polymorphic purity during synthesis and crystallization of clopidogrel bisulfate Form I by identifying Form II during batch drug product crystallization in real time.

ASSOCIATED CONTENT

Supporting Information

The Supporting Information is available free of charge on the ACS Publications website at DOI: 10.1021/acs.analchem.7b00431.

Method for aligning bright field (BF) images and second harmonic generation (SHG) images acquired by the SONICC system (Formulatrix Inc.) (PDF)

AUTHOR INFORMATION

Corresponding Author

*E-mail: gsimpson@purdue.edu.

ORCID

Srividya Ramakrishnan: 0000-0002-7892-994X

Garth J. Simpson: 0000-0002-3932-848X

Notes

The authors declare no competing financial interest.

ACKNOWLEDGMENTS

The authors gratefully acknowledge financial support from the National Science Foundation GOALI award entitled "Informing Amorphous Formulations Design through Quantitative Nonlinear Optical Analysis", Grant No. 1412888-CHE.

REFERENCES

(1) Aaltonen, J.; Allesø, M.; Mirza, S.; Koradia, V.; Gordon, K. C.; Rantanen, J. *Eur. J. Pharm. Biopharm.* **2009**, *71*, 23−37.

(2) Chieng, N.; Rades, T.; Aaltonen, J. *J. Pharm. Biomed. Anal.* **2011**, *55*, 618−644.

(3) Singhal, D.; Curatolo, W. *Adv. Drug Delivery Rev.* **2004**, *56*, 335−347.

(4) Snider, D. A.; Addicks, W.; Owens, W. *Adv. Drug Delivery Rev.* **2004**, *56*, 391−395.

(5) Bauer, J.; Spanton, S.; Henry, R.; Quick, J.; Dziki, W.; Porter, W.; Morris, J. *Pharm. Res.* **2001**, *18*, 859−866.

DOI: 10.1021/acs.analchem.7b00431
Anal. Chem. 2017, 89, 5958−5965

(6) Chieng, N.; Rades, T.; Aaltonen, J. *J. Pharm. Biomed. Anal.* **2011**, *55*, 618−644.
(7) Bousquet, A.; Castro, B.; Saint-Germain, J. *Polymorphic clopidogrel hydrogenesulphate form*. U.S. Patent 6,429,210, August 6, 2002.
(8) Lu, J.; Wang, J.; Rohani, S. *Cryst. Res. Technol.* **2012**, *47*, 505−510.
(9) Nemet, Z.; Demeter, A.; Pokol, G. *J. Pharm. Biomed. Anal.* **2009**, *49*, 32−41.
(10) Badorc, A.; Frehel, D. *Dextrorotatory enantiomer of alpha-(4,5,6,7-tetrahydrothieno[3,2-c]pyrid-5-yl)(2-chlorophenyl)methyl acetate, process for its preparation and pharmaceutical compositions containing it*. EP Patent EP0281459 A1, September 7, 1988.
(11) Koradia, V.; Chawla, G.; Bansal, A. K. *Acta Pharm.* **2004**, *54*, 193−204.
(12) Fahr, A.; Liu, X. *Expert Opin. Drug Delivery* **2007**, *4*, 403−416.
(13) Raw, A. *Adv. Drug Delivery Rev.* **2004**, *56*, 235−236.
(14) Raw, A. S.; Furness, M. S.; Gill, D. S.; Adams, R. C.; Holcombe, F. O., Jr.; Yu, L. X. *Adv. Drug Delivery Rev.* **2004**, *56*, 397−414.
(15) Uvarov, V.; Popov, I. *J. Pharm. Biomed. Anal.* **2008**, *46*, 676−682.
(16) Raijada, D. K.; Prasad, B.; Paudel, A.; Shah, R. P.; Singh, S. *J. Pharm. Biomed. Anal.* **2010**, *52*, 332−344.
(17) Yin, X. Z.; Xiao, T. Q.; Nangia, A.; Yang, S.; Lu, X. L.; Li, H. Y.; Shao, Q.; He, Y.; York, P.; Zhang, J. W. *Sci. Rep.* **2016**, *6*, 24763.
(18) Wanapun, D.; Kestur, U. S.; Kissick, D. J.; Simpson, G. J.; Taylor, L. S. *Anal. Chem.* **2010**, *82*, 5425−5432.
(19) Toth, S.; Madden, J.; Taylor, L.; Marsac, P.; Simpson, G. *Anal. Chem.* **2012**, *84*, 5869−5875.
(20) Toth, S. J.; Schmitt, P. D.; Snyder, G. R.; Trasi, N. S.; Sullivan, S. Z.; George, I. A.; Taylor, L. S.; Simpson, G. J. *Cryst. Growth Des.* **2015**, *15*, 581−586.
(21) Chowdhury, A. U.; Dettmar, C. M.; Sullivan, S. Z.; Zhang, S.; Jacobs, K. T.; Kissick, D. J.; Maltais, T.; Hedderich, H. G.; Bishop, P. A.; Simpson, G. J. *J. Am. Chem. Soc.* **2014**, *136*, 2404−2412.
(22) Hall, V. J.; Simpson, G. J. *J. Am. Chem. Soc.* **2010**, *132*, 13598−13599.
(23) Schmitt, P. D.; DeWalt, E. L.; Dow, X. Y.; Simpson, G. J. *Anal. Chem.* **2016**, *88* (11), 5760−5768.
(24) Newman, J. A.; Schmitt, P. D.; Toth, S. J.; Deng, F.; Zhang, S.; Simpson, G. J. *Anal. Chem.* **2015**, *87* (21), 10950−10955.
(25) Chowdhury, A. U.; Zhang, S.; Simpson, G. J. *Anal. Chem.* **2016**, *88* (7), 3853−3863.
(26) Wu, L.; Vogt, F. G. *J. Pharm. Biomed. Anal.* **2012**, *69*, 133−147.
(27) Simpson, G. J. *Nonlinear Optical Polarization Analysis in Chemistry and Biology*; Cambridge University Press: New York, 2017.
(28) Haupert, L. M.; DeWalt, E. L.; Simpson, G. J. *Acta Crystallogr., Sect. D: Biol. Crystallogr.* **2012**, *68*, 1513−1521.
(29) Madden, J. T.; Toth, S. J.; Dettmar, C. M.; Newman, J. A.; Oglesbee, R. A.; Hedderich, H. G.; Everly, R.; Becker, M.; Ronau, J. A.; Buchanan, S. K. *J. Synchrotron Radiat.* **2013**, *20*, 531−540.
(30) Newman, J. A.; Zhang, S.; Sullivan, S. Z.; Dow, X. Y.; Becker, M.; Sheedlo, M. J.; Stepanov, S.; Carlsen, M. S.; Everly, R. M.; Das, C. *J. Synchrotron Radiat.* **2016**, *23*, 959−965.
(31) Otsu, N. *Automatica* **1975**, *11*, 23−27.
(32) Harris, D. C.; Bertolucci, M. D. *Symmetry and Spectroscopy: An Introduction to Vibrational and Electronic Spectroscopy*; Courier Corporation: New York, 1978.
(33) Cardew, P.; Davey, R. *Proc. R. Soc. London, Ser. A* **1985**, *398*, 415−428.
(34) Parrinello, M.; Rahman, A. *J. Appl. Phys. (Melville, NY, U. S.)* **1981**, *52*, 7182−7190.

DOI: 10.1021/acs.analchem.7b00431
Anal. Chem. 2017, 89, 5958−5965